Effect of Rotating Earth for Analysis of Aeroassisted Orbital Transfer Vehicles

Hideo Ikawa*
Aerojet Propulsion Research Institute, Sacramento, California

Aeroassisted orbital transfer vehicles operate both in the endo- and exo-atmospheres. Although an orbital trajectory is shaped by the inertial state variables, the aerodynamic maneuvering that induces trajectory perturbation is dictated by the relative velocity. The difference in relative velocities between a nonrotating and a rotating earth produces a substantial difference in the entry dynamic pressure. The exit-condition errors introduced at the edge of sensible atmosphere by the dynamic pressure difference produce significant deviations in the final orbit transfer. Endo-atmospheric flight control laws that tend to minimize the orbit reinsertion propellent requirement for orbit transfer and plane change are also demonstrated. In conclusion, aeroassisted orbital transfer vehicle analysis with an operational altitude constraint and a stationary earth assumption tends to underpredict the final low-earth orbit altitude and to overpredict the orbital inclination change. Because the turning radius is on the order of a global scale, latitude positions may influence the effectiveness of orbit plane-change analysis.

Nomenclature

$AOTV$	= aeroassisted orbital transfer vehicle
Az	= heading azimuth, deg
C_2, C_3	= coefficients defined by Eq. (4)
D,L	= aerodynamic drag and lift, N
F_1,F_2,F_3	= coefficients defined by Eq. (5)
H_{orb}	= desired orbit altitude, km
i	= trajectory inclination, deg
L/D	= lift over drag ratio
m	= vehicle mass, kg
r	= radius altitude, km
R_a,R_p	= apogee, perigee radii, km
R_b	= normalized radius = R_a/r
Re	= earth's mean radius, km
R_{orb}	= targetted orbit radius, Km
Q	= normalized velocity parameter by Eq. (11)
T	= thrust, N
V	= relative velocity, km/s
V_a,V_p	= apogee, perigee velocity, km/s
V_{ca}	= circular velocity at apogee, km/s
V_i	= inertial velocity, km/s
α	= angle of attack, deg
α_T	= thrust angle, deg
β	= bank angle, counterclockwise positive, deg
γ	= flight path angle, positive up, deg
θ	= downrange angle, deg
μ	= gravitational constant, km^3/s^2
ϕ	= cross-range angle, deg
ϕ_L	= latitude, deg
ψ	= heading angle, positive left, deg
ω_E	= earth's rotational rate, deg/s

Subscripts

i	= inertial properties
0	= initial position

Presented as Paper 86-2133 at the AIAA Flight Mechanics Conference, Williamsburg, VA, Aug. 18-20, 1986; received May 19, 1986; revision received March 23, 1987.

*Senior Research Scientist. Presently Senior Technical Specialist, Northrop Aircraft, Hawthorne, CA. Member AIAA.

Introduction

In the past few years, the concept of aeroassisted orbital transfer vehicles (AOTV) that may satisfy economical and reusable requirements has been investigated by many researchers. For analytical simplicity, however, an idealized nonrotating earth has been used as the frame of reference for trajectory simulation and optimization studies,[1-4] except those in which the POST program has been applied.[5,6] The preceding approach is acceptable for preliminary investigations of the aeroassisted orbital transfer vehicle concept. The realistic trajectory simulations of low-earth orbit transfer are significantly affected by the earth's rotation during the endo-atmospheric flight phase.

In this paper, the possible discrepancies that may be introduced in analyses by neglecting the earth's rotation are discussed. The entire transfer trajectory from a deorbiting altitude to reach a low-earth-orbit reinsertion altitude is accomplished with the unpowered maneuver. However, the aerodynamic contributions that influence the shaping of ascent glide trajectory from the maneuvering altitude to the edge of sensible atmosphere are unknown a priori. Therefore, a minimum propellent trajectory is defined by the unpowered endo-atmospheric glide trajectory that minimizes the reinsertion burn propellent expenditure at the low-earth orbit. A simplified technique that determines a proper glide angle and the exit conditions to satisfy the foregoing requirement is discussed.

The turning radius of an orbital plane-change maneuver is in the same order of magnitude as the earth's radius of a few thousand kilometers; this requires spherical geometric consideration in analysis. In this case, the latitude position usually ignored in the simplified formulation[1-4] contributes to the effectiveness of orbital inclination change.

Methodology

Governing Equations

The following assumptions are made for the aeroassisted orbital transfer vehicle concept: 1) the primary purpose is to dissipate high-orbit-altitude potential energy by aerodynamic deceleration in lieu of the propulsive method, 2) most of the orbit plane change is performed by aerodynamic maneuver, and 3) the vehicle is space-based and remains in a low-earth orbit.

For realistic investigations of this concept, a rotating earth system must be considered. For example, the shaping of an exo- and endo-atmospheric trajectory is dictated by the inertial state variables of the equation of motion. However, trajectory perturbation induced by aerodynamic maneuvering is influenced by the relative velocity components between a vehicle and the atmosphere that are assumed to be rotating with the earth. For the sake of completeness, the full equations of motion, as derived in Ref. 7, are presented.

$$\frac{dV}{dt} = [T\cos(\alpha_T+\alpha) - D]/m - \mu\sin\gamma/r^2 + r\omega_E^2 F_1 \tag{1}$$

$$V\frac{d\gamma}{dt} = [T\sin(\alpha_T+\alpha) + L]\cos\beta/m - (\mu/r^2 - V^2/r)\cos\gamma + 2V\omega_E C_2 + r\omega_E^2 F_2 \tag{2}$$

$$V\cos\gamma\frac{d\psi}{dt} = [T\sin(\alpha_T+\alpha) + L]\sin\beta/m - V^2\cos^2\gamma\cos\psi\tan\phi/r - 2V\omega_E C_3 - r\omega_E^2 F_3 \tag{3}$$

where

$$C_2 = \cos i_0\cos\phi\cos\psi - \sin i_0[\sin\psi\cos(\theta_0+\theta) + \cos\psi\sin\phi\sin(\theta_0+\theta)] \tag{4a}$$

$$C_3 = \cos i_0(\cos\gamma\sin\phi - \sin\gamma\cos\phi\sin\psi) + \sin i_0[(\cos\gamma\cos\phi + \sin\gamma\sin\phi\sin\psi)\sin(\theta_0+\theta) - \sin\gamma\cos\psi\cos(\theta_0+\theta)] \tag{4b}$$

and

$$F_1 = [\cos^2 i_0 + \sin^2 i_0\cos^2(\theta_0+\theta)]\cos\phi(\sin\gamma\cos\phi - \cos\gamma\sin\phi\sin\psi) + \sin^2 i_0[\sin\phi(\sin\gamma\sin\phi + \cos\gamma\cos\phi\sin\psi) - \cos\gamma\cos\phi\cos\psi\cos(\theta_0+\theta)\sin(\theta_0+\theta)] - \sin i_0\cos i_0[\cos\gamma\cos\psi\sin\phi\cos(\theta_0+\theta) + (2\sin\gamma\sin\phi\cos\phi + \cos\gamma\sin\psi\cos 2\phi)\sin(\theta_0+\theta)] \tag{5a}$$

$$F_2 = [\cos^2 i_0 + \sin^2 i_0\cos^2(\theta_0+\theta)]\cos\phi(\cos\gamma\cos\phi + \sin\gamma\sin\phi\sin\psi) + \sin^2 i_0[\sin\phi(\cos\gamma\sin\phi - \sin\gamma\cos\phi\sin\psi) + \sin\gamma\cos\phi\cos\psi + \cos(\theta_0+\theta)\sin(\theta_0+\theta)] + [\sin i_0\cos i_0\{\sin\gamma\sin\phi\cos\psi\cos(\theta_0+\theta) + [\sin\gamma\sin\psi - 2\sin\phi(\cos\gamma\cos\phi + \sin\gamma\sin\phi\sin\psi)]\sin(\theta_0+\theta)\} \tag{5b}$$

$$F_3 = \cos^2 i_0\sin\phi\cos\phi\cos\psi - \sin^2 i_0\cos\phi[\sin\psi\sin(\theta_0+\theta)\cos(\theta_0+\theta) + \sin\phi\cos\psi\sin^2(\theta_0+\theta)] + \sin i_0\cos i_0[\cos\psi\cos 2\phi\sin(\theta_0+\theta) - \sin\phi\sin\psi\cos(\theta_0+\theta)] \tag{5c}$$

In addition, the kinematic equations are given as

$$\frac{dr}{dt} = V\sin\gamma \tag{6}$$

$$\frac{d\theta}{dt} = V\cos\gamma\cos\psi/r\cos\phi \tag{7}$$

$$\frac{d\phi}{dt} = V\cos\gamma\sin/r \tag{8}$$

The trajectory inclination angle changes only when aerodynamic and/or propulsive force components are applied in the lateral direction of motion. The rate of inclination change is defined in terms of azimuth, latitude position, and the rate of heading angle change as induced by external forces [first right-hand term of Eq. (3)]. It is most effective across an equatorial crossing. For some of the maximum lift-over-drag-ratio flight, a turning maneuver results in a long down range traverse on a spherical planet. In some cases, the flight can be extended over the apex of the inclined orbit where the rate of inclination change is most ineffective, but the rate of nodal change is most effective. In fact, in order to maintain a monotonically increasing or decreasing trajectory inclination, it is necessary to switch the bank angle (e.g., a bank angle of +90 to −90 deg) at the trajectory apex.[7] The auxiliary inclination change equation is defined as

$$\frac{di}{dt} = \left(\frac{\cos Az\cos\phi_L}{\sin i}\right)\left(\frac{d\psi}{dt}\right)_{EF} \tag{9}$$

where $(d\psi/dt)_{EF}$ is given by the first right hand term of thrust and lift of Eq. 3.

Transformations of the variables between the relative and inertial properties depend on the trajectory inclination, radius altitude, and latitude position. The transformations for velocity and flight path angle are given as

$$V_i^2 = V^2 + 2Vr\omega_E\cos\gamma\cos i + (r\omega_E\cos\phi_L)^2 \tag{10a}$$

$$V_i\sin\gamma_i = V\sin\gamma \tag{10b}$$

The nonrotating earth problem can be solved by setting the earth's rotational rate term (ω_E) equal to zero in Eqs. (1-3) and in Eq. (10). For the rotating earth problem, the state variables are defined relatively with respect to an observer fixed on a rotating planet. In this case, the total system is defined by inclusion of acceleration terms induced by the planet's rotation [Eqs. (4) and (5)].

The primary concern for the aeroassisted orbital transfer vehicle analysis is an ability to properly define the exit conditions for orbit reinsertion that can be influenced by the dynamic pressure difference between two reference systems. For example, the velocity difference between the inertial and the relative reference systems as taken along the equatorial flight path is aproximately 500 m/s, which represents 5 to 7% of the entry velocity. In terms of dynamic pressure, the difference becomes 10 to 14% of the entry dynamic pressure, which is nonnegligible in determining the ultimate orbit. The orbital transfer discrepancies induced by the velocity difference, therefore, may be far greater than the correction that could be applied by optimization using the inertial reference frame system.

Aeroassisted Orbit Transfer Vehicle Configuration

In returning from a high-energy orbit, the aerodynamic deceleration for low-earth orbit transfer and the glide maneuver for plane change will be accomplished in a relatively short period. For example, the unpertubative elliptic orbit transfer from a geosynchronous orbit to a perigee altitude of

76.2 km (250 kft) takes approximately 6 hours. The orbit transfer vehicle, however, resides within the sensible atmosphere below 122 km (400 kft) for only a period of approximately 220 s and for an enclosed sweep angle of 21 deg (Fig. 1), provided that no aerodynamic deceleration is applied.

The 76.2 km perigee altitude is chosen because the aeroheating becomes excessive if the entry vehicle penetrates below this altitude. This imposes stringent requirements for a vehicle design having low ballistic coefficient and high lift-over-drag ratio capabilities. Fortunately, based on the prior assumption of space-based operation, the aeroassisted orbit transfer vehicle configuration can be tailored only for hypersonic operations above Mach 20, and the conventional planform for low-speed maneuver can be neglected.

For simplicity, a configuration having a double-wedge lower surface and a flat upper surface is selected for the baseline study. The upper surface is taken as the reference plane. The aerodynamic coefficients are estimated using the Newtonian theory without applying the viscous interaction.[8] The aerodynamic coefficients are shown in Fig. 2. The maximum lift-over-drag ratio occurs at the -5 deg angle of attack. It will be shown later that the optimal angle of attack for the aeroassisted plane-change maneuver occurs in regions above the angle of attack for the maximum L/D. Of course, the optimal angle of attack shifts toward the maximum L/D as lower operational altitude is considered where aerodynamics become more effective. The aeroheating constraint, however, may preclude the lower altitude maneuvers.

Exit Conditions

For the aeroassisted orbital transfer vehicle concept, three-dimenional trajectory simulation to reach a prescribed low-earth orbit altitude must satisfy the following combination of exit conditions at the edge of sensible atmosphere: 1) exit velocity, 2) exit-flight path angle, and 3) required orbit inclination change. If the lift component in the lateral direction is insufficient for the orbital inclination change, then the remaining plane-change requirement must be met propulsively at the initial deorbiting altitude during the retro-burn.

A minimum ΔV for reinsertion burn for low-earth orbit circularization can be achieved if the exit-flight path angle is maintained near zero. The requirements can be estimated by using Keplerian mechanics. The elliptic orbital elements are described by the following set of equations.

The normalized exit inertial velocity parameter is defined as

$$Q = rV_i^2/\mu \tag{11}$$

Then, the eccentricity of transfer orbit can be given as

$$e = \sqrt{1 - Q(2-Q)\cos^2\gamma_i} \tag{12}$$

The radii and velocities of apogee and perigee are

$$R_a, R_p = (1 \pm e)r/(2-Q) \tag{13}$$

$$V_a, V_p = (1 \mp e)\sqrt{\mu/Qr}\cos\gamma_i \tag{14}$$

where the upper signs apply to the first left-hand parameters.

To determine the matched exit conditions to reach a prescribed orbit, let us define a normalized radius (R_b) by a ratio of a desired orbit radius (equals an apogee radius, R_a) and an exit radius (r). For a fixed R_b, the velocity parameter (Q) as given in Eq. (11) can be reformulated by manipulating the apogee radius equation, Eq. (13). Then, the parameter Q is defined by the local function of the inertial flight path angle (γ_i).

$$R_b = R_a/r \tag{15}$$

$$Q(R_b, \gamma_i) = 2R_b(R_b - 1)/(R_b^2 - \cos^2\gamma_i) \tag{16}$$

If we substitute Q into Eqs. (11–14) inclusively, then the required orbit transfer parameters can be mapped with respect to the ΔV. The ΔV is determined by taking the difference of circular (V_{ca}) and transfer (V_a) velocities, both defined at the apogee altitude as

$$V_{ca} = \sqrt{\mu/R_a} \tag{17}$$

$$\Delta V_a = V_{ca} - V_a \tag{18}$$

The orbit transfer prameters for the exit altitude of 122 km and the targeted circular orbit altitude of 305 km are shown in

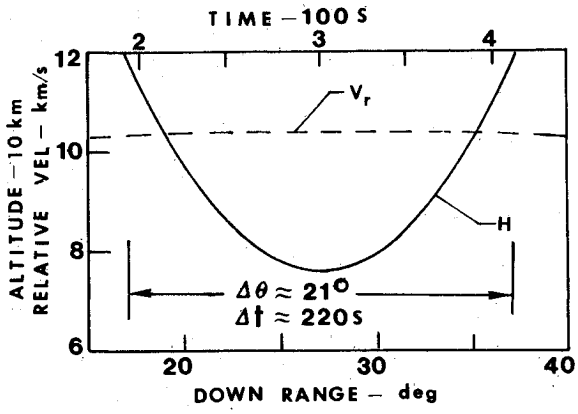

Fig. 1 Endo-atmospheric residence time and range, without aerodynamics. Transfer from geosynchronous earth orbit to 76.2 km perigee altitude.

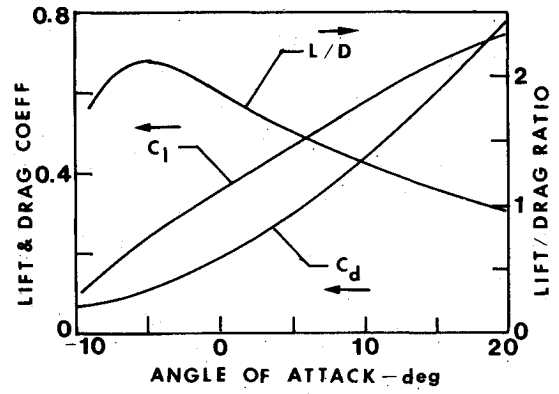

Fig. 2 A double-wedge aeroassisted orbit transfer vehicle. Aerodynamic data: Entry weight = 7273 kg; reference area = 93 m^2.

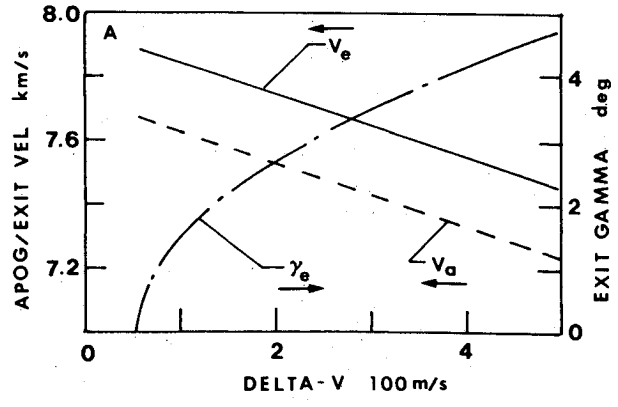

Fig. 3 Orbit transfer parameters vs required apogee ΔV. Exit altitude = 122 km; target altitude = 305 km.

Fig. 3. The absolute minimum ΔV requirement is 54 m/s. Although it is very difficult to satisfy the "zero exit-flight path angle requirement," it is encouraging to note that less than 80 m/s of ΔV can be met with the exit-flight path angle of up to 1 deg.

Endo-Atmospheric Flight Control Law

The aeroassisted orbital transfer vehicle trajectory optimization has been formulated by many investigators using the variational technique. However, the convergence of solution depends highly on the accuracy of the nominal trajectory. In the present study, a simple control law is derived by an application of known facts.

As noted, a minimum propellent of reinsertion burn for a transfer trajectory can be achieved by satisfying the near-zero flight path angle at the exit edge of sensible atmosphere. However, this condition may be difficult to meet because the endo-atmospheric flight is unpredictable, and the departing conditions from the gliding maneuver are unknown a priori.

One approach to finding the near optimal glide trajectory in the atmosphere is to follow a shallow glide path angle that is prescribed near the perigee altitude. An angle of attack is held constant and the vehicle is controlled by a bank angle modulation. By setting the left-hand term of Eq. (2) to zero, the required bank angle is solved. This mode of operation is identified as a shallow glide path ascent trajectory.

For a given angle-of-attack flight, the apogee radius (R_a) of transfer orbit is computed by Eqs. (11-13) as functions of locally known altitude, inertial velocity, and glide path angle. The computed R_a value decays during the endo-atmospheric flight and approaches a constant as the vehicle leaves the atmosphere. The difference between the radii of desired orbit (R_{orb}) and the computed apogee (R_a) is monitored during the trajectory simulation. The proper glide path angle can be found by performing an iteration only between the operational and the exit altitudes until the monitored ΔR_{orb} approaches zero (Fig. 4).

Although the foregoing technique produces a trajectory for a minimal propellent reinsertion burn, a plane change during the endo-atmospheric flight phase is not maximized. As felt intuitively and shown by an optimization study, more effective turning may be achieved if the vehicle maintains a 90 deg bank angle. Unfortunately, this condition may not always be satisfied if the operational altitude is constrained.

The control mode defined by the constant altitude glide trajectory in atmosphere, a limiting case of the one previously discussed, may produce better turning results. However, reorbiting requires a pull-up maneuver whereby the point of departure can be determined by monitoring the R_a value as given by Eq. (13).

The technique discussed here is applicable for both stationary and rotating earth trajectory simulations because Eq. (13) is defined by the inertial velocity that is related by Eq. (10). The same technique can also be used for a simulation of boost ascent trajectory to orbit.

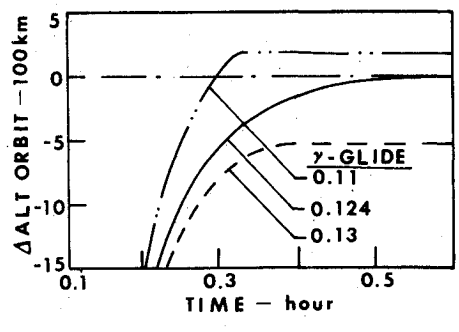

Fig. 4 Typical glide path iteration: Orbital altitude vs time.

Results and Discussion

In order to demonstrate the importance of rotating earth contribution on aeroassisted orbital transfer vehicle trajectory analysis, the following comparisons are made. A hypothetical transfer vehicle with an entry weight of 7273 kg (16,000 lb), a reference area of 93 m 1000 ft, and aerodynamic characteristic data as given in Fig. 2 is assumed. The 1962 U.S. Standard Atmospheric data are used.

Without Aerodynamic Modulation

To assess the unbiased results of trajectory comparison, both trajectories for stationary and rotating earth cases are simulated with the aerodynamic characteristics defined at an angle of attack of 20 deg (Fig. 2). A 90 deg bank angle is maintained during the atmospheric glide phase so that the lift component acts only in the direction of orbital plane change. The final shaping of a low-earth orbit transfer, therefore, is dictated only by the deviation in aerodynamic drag induced by the dynamic pressure difference.

The altitude and inertial velocity histories below 110 km in altitude are compared in Fig. 5a to delineate the details of

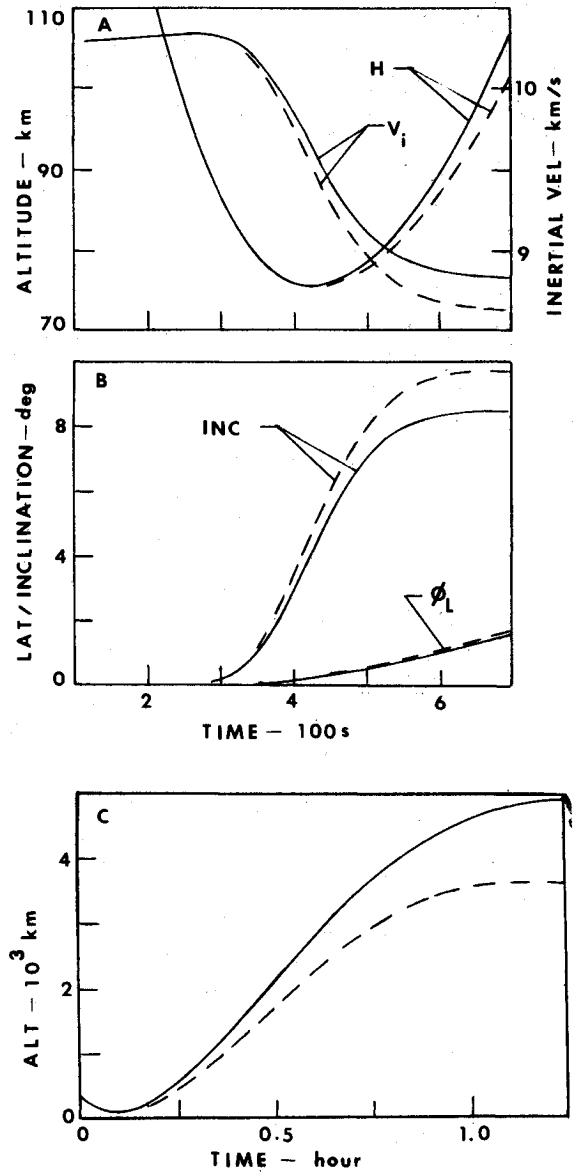

Fig. 5 Constant attitude aeroassisted orbit transfer vehicle trajectory histories; $\alpha = 20$ deg; $\beta = 90$ deg: a) Endo-atmospheric glide altitude and inertial velocity, b) Inclination, latitude, c) Altitude in low-earth orbit transfer. Broken line indicates the stationary earth, solid line indicates rotating earth.

aerodynamic contribution. The noticeable deviation in velocity history appears near the altitude of 80 km during the descent. The stationary earth trajectory shows a greater deceleration effect because of experiencing a higher dynamic pressure history. Hence, the lower altitude and velocity histories (Fig. 5a) and more effective turning capability (Fig. 5b) are demonstrated by this case.

The final exo-atmospheric trajectories are compared in Fig. 5c. A deviation in exit conditions affects the ultimate reinsertion orbits. The final orbit transfer error introduced by the stationary earth assumption is significant. It tends to underpredict the final altitude and to overpredict the orbit inclination change as compared to the rotating earth case.

Shallow Glide Path Ascent Trajectory

As discussed in the methodology section, an efficient propellent orbit transfer can be achieved by a shallow glide in the atmosphere using a bank angle modulation. A targeted low-earth orbit altitude is arbitrarily selected at 274.5 km (900 kft). The angle of attack is set at 8 deg. For a stationary earth case, an unpowered glide path angle of 0.1327 deg attains the desired low-earth orbit transfer. For a comparison, the same angle of attack and glide path angle are used for a rotating earth case. The bank angle is modulated to satisfy the zero flight-path derivative in Eq. (2).

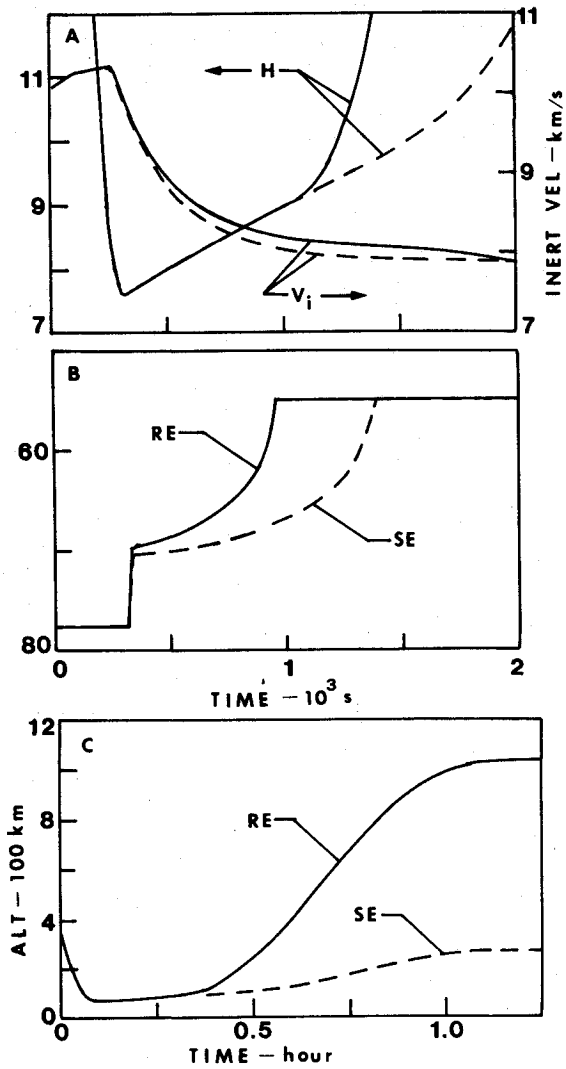

Fig. 6 Shallow glide path ascent trajectory histories; $\alpha = 8$ deg, bank modulated; γ glide = 0.1327 deg: a) Endo-atmospheric glide altitude and inertial velocity, b) Bank angle, c) Altitude in low-earth transfer. Broken line indicates the stationary earth, solid line indicates rotating earth.

The altitude and inertial velocity histories are shown in Fig. 6a. The rotating earth trajectory deviates away from the prescribed glide path before the stationary earth case. The reason for this behavior can be explained by the bank histories (Fig. 6b). The initial atmospheric descent is accomplished with a 90 deg bank until it reaches the prescribed glide path. From this point and beyond, the vehicle begins to ascend due to centrifugal force induced by the supervelocity. Since the counterbalancing force is proportional to a product of lift and the cosine of bank angle, a bank modulation of greater than 90 deg is initiated. The rotating earth case requires a larger bank angle history to compensate for the effect of reduced dynamic pressure. As the vehicle ascends, it reaches a point where it is no longer able to maintain the prescribed glide path angle because of insufficient negative aerodynamic lift, even with a fully inverted attitude. At this point, the flight equilibrium is violated and the vehicle leaves the proper glide path.

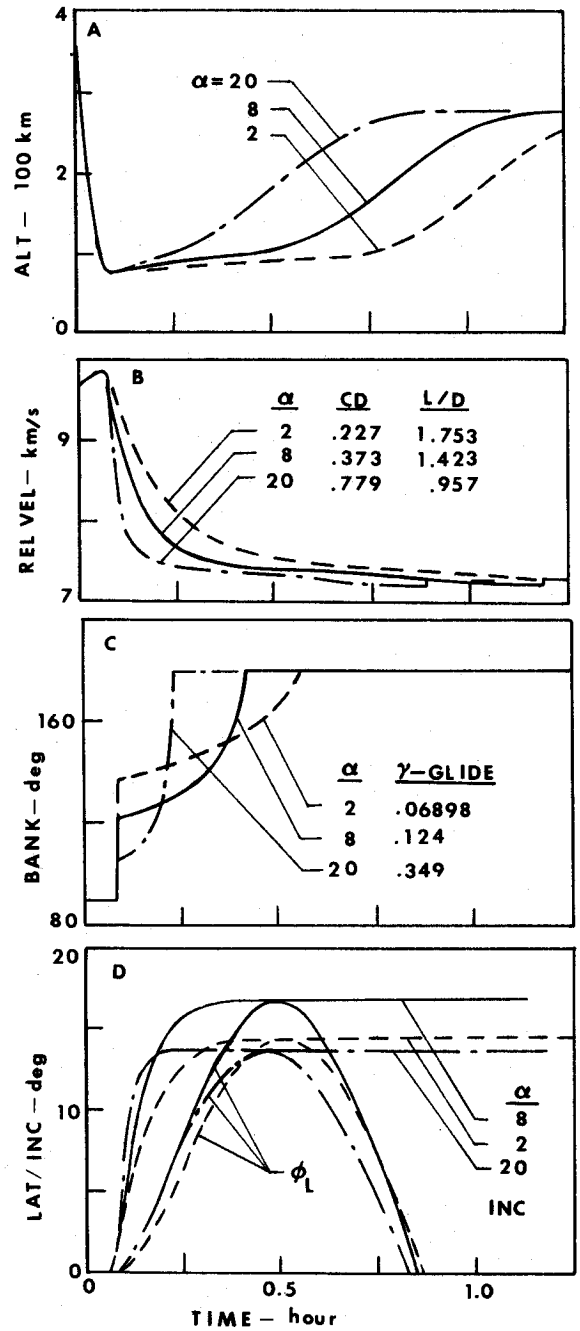

Fig. 7 Effects of angle of attack for rotating earth, shallow glide path ascent trajectory histories; $\Delta V_{orb} = 51.6$ m/s: a) Altitude, b) Relative velocity, c) Blank angle, and d) Inclination, latitude.

The variation in a pair of velocity and flight-path angle at the exit altitude produces a considerably different final orbit, as depicted in Fig. 6c. This implies that the orbit transfer conditions defined by the stationary earth consideration do not satisfy the actual conditions. Consider a feedback system that is designed to follow an endo-atmospheric nominal trajectory established by the stationary earth system. If this system is applied to the actual rotating earth system, the error induced in the atmospheric exit conditions places the vehicle on a transfer ellipse having a considerably different apogee.

Angle-of-Attack Effects

Many combinations of angles of attack and glide path angles exist to equally satisfy the predefined low-earth orbit transfer from a given perigee altitude. Angles of attack from 2 to 20 deg are investigated for the realistic rotating earth case. The glide path is selected by the aforementioned iteration technique.

The altitude histories and the relative velocity histories are compared in Figs. 7a and 7b, respectively. The ΔV for the orbit circularization is 51.6 m/s (± 1 m/s) for all cases. The bank angle histories are shown in Fig. 7c. A 2 deg angle-of-attack case initially requires the greatest bank angle modulation. This is because a smaller angle of attack with a higher lift over drag ratio may necessarily produce an insufficient lift for control and turning maneuvers. However, it can be modulated for a longer duration due to a slower deceleration. The converse is true for a glide with a 20 deg angle-of-attack case.

Obviously, there exists an optimal angle of attack that maximizes the orbital inclination change. It must be noted that definitions of inclination change, and turning angle maneuvers are not synonymous [Eq. (9)]. A maximum inclination change of 16.7 deg is obtained by an 8 deg angle-of-attack trajectory (Fig. 7d). Two deg angle-of-attack data show that the latitude position reaches the upper apex during the atmospheric flight that degrades the inclination change capability.

Angle-of-Attack Effects for a Constant Altitude Glide

The effect of varying angles of attack during a constant altitude glide maneuver is investigated. The descent from the entry to the perigee is accomplished by maintaining a constant flight attitude of a 1 deg angle of attack and a 90 deg bank angle. As noted in Fig. 2, the maximum L/D occurs at the -5 deg angle of attack. However, for an angle of attack below -3 deg, an insufficient lift exists to maintain a flight along the 0 deg glide path. A point of pull-up maneuver is iterated. The exit-flight path is greater than the previous mode that penalizes the reinsertion ΔV.

The desired low-earth orbit insertion is accomplished with a ΔV of 118.9 m/s. The maximum inclination change of 22.36 is attained by the zero angle-of-attack case.

Table 1 Total ΔV requirements for $\Delta i = 28.5$ deg

Mode	Shallow glide	Constant altitude glide
Δi (space)	11.78 deg	6.14 deg
Δi (aero)	16.72 deg	22.36 deg
Δi (total)	28.50 deg	28.50 deg
ΔV (space)	1558.4 m/s	1509.6 m/s
ΔV (aero)	51.6 m/s	118.8 m/s
ΔV (total)	1610.0 m/s	1628.4 m/s

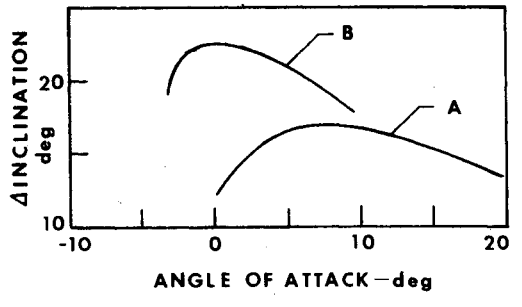

Fig. 8 Summary of orbit inclination change vs angle of attack: a) Shallow glide path ascent trajectory and b) Constant altitude glide trajectory.

Summary

A summary of inclination change vs angle of attack is depicted in Fig. 8. The optimal angle of attack is 8 deg for the shallow glide path ascent trajectory and 0 deg for the constant altitude glide trajectory. It is interesting to note that for a total ΔV capability of a 28.5 deg plane change from a geosynchronous orbit to a low-earth orbit transfer, the shallow glide path ascent trajectory mode is found superior to the constant altitude glide trajectory mode as summarized in Table 1.

Conclusion

Possible trajectory simulation errors introduced by neglecting the earth's rotation in the endo-atmospheric glide phase have been demonstrated for aeroassisted orbital transfer vehicle analysis. A difference of 10 to 14% in entry dynamic pressure may alter the exit conditions sufficiently enough to introduce significant deviations in orbit transfer simulation. Because the turning radius is on the order of a global scale, the latitude traverse during the orbital inclination change maneuver is also nonnegligible, especially for a high lift over drag ratio flight. A simple endo-atmospheric flight control law using a bank angle modulation has effectively simulated efficient propellent orbit transfers.

Future optimization study of aeroassisted orbital transfer vehicle trajectory should include the earth's rotational contribution in the endo-atmospheric flight analysis. Otherwise, nominal trajectories generated by the method using a nonrotating earth may underpredict the final orbital altitude and overpredict the orbital inclination change.

References

[1]Mease, K.D. and Vinh, N.X., "Minimum-Fuel Aeroassisted Coplanar Orbit Transfer Using Lift Modulation," *Journal of Guidance, Control, and Dynamics,* Vol. 8, Jan.-Feb. 1985, pp. 134-141.

[2]Johannesen, J.R., Vinh, N.X., and Mease, K.D., "Effect of Maximum Lift to Drag Ratio on Optimal Aeroassisted Plane Change," AIAA Paper 85-1817; also, 12th Atmospheric Flight Mechanics Conference, Snowmass, CO., Aug. 19-20, 1985.

[3]Mease, K.D. and McCreary, F.A., "Atmospheric Guidance Law for Planar Skip Trajectory," AIAA Paper 85-1818; also, 12th Atmospheric Flight Mechanics Conference, Snowmass, CO, Aug. 19-21, 1985.

[4]Hull, D.G, "New Analytical Results for AOTV Guidance," AIAA Paper 85-1820; also, 12th Atmospheric Flight Mechanics Conference, Snowmass, CO., Aug. 19-21, 1985.

[5]Rehder, J.J., "Multiple Pass Trajectory for an Aeroassisted Orbit Transfer Vehicle," "Thermal Design of Aeroassisted Orbit Transfer Vehicle," *Progress in Astronautics and Aeronautics,* Vol. 96, 1985, pp. 186-197.

[6]Taley, T.A., White, N.H., and Naftel, J.C., "Impact of Atmospheric Uncertainties and Viscous Interaction Effects on the Performance of Aeroassisted Orbit Transfer Vehicle," *Progress in Astronautics and Aeronautics,* Vol. 96, 1985, pp. 198-229.

[7]Ikawa, H., "A Unified Three-Dimensional Trajectory Simulation Methodology," *Journal of Guidance, Control, and Dynamics,* Vol. 9, Nov.-Dec. 1986, pp. 650-656.

[8]Lees, L, "Hypersonic Flow," *IAS-RAeS Proceedings,* 1955, pp. 241-276.